Comparison of Hartree-Fock and density functional theory structure factors and charge density in diamond, silicon and germanium

1999 J. Phys.: Condens. Matter 11 5827

(http://iopscience.iop.org/0953-8984/11/30/312)

J. Phys.: Condens. Matter **11** (1999) 5827–5843. Printed in the UK PII: S0953-8984(99)99040-9

Comparison of Hartree–Fock and density functional theory structure factors and charge density in diamond, silicon and germanium

Joël Pere, Michel Gelizé-Duvignau and Albert Lichanot

Laboratoire de Chimie Structurale—UMR 5624, Université de Pau et des Pays de l'Adour, IFR, rue Jules Ferry, 64000 Pau, France

Received 6 November 1998, in final form 19 April 1999

Abstract. Crystalline orbitals of diamond, silicon and germanium have been calculated using the linear combination of atomic orbitals–self-consistent-field method as implemented in the CRYSTAL 95 program. The calculations have been carried out to the Hartree–Fock and density functional levels of theory with two formulations of the exchange–correlation potential correcting the electronic density.

The static and room temperature structure factors and charge densities have been deduced and compared with the available experimental data and other calculations. The effects of the exchange and correlation potentials are evaluated and the change of the charge density is discussed in connection with the thermal motion.

1. Introduction

Diamond, silicon and germanium are typical covalent crystals in which each atom is linked tetrahedrally to four neighbouring atoms. Their electronic structure has been accurately refined in crystallography over the past two decades using the x-ray Pendellosung-beat method on large single crystals. High-quality structure factors are available, particularly for silicon where 31 reflections have been investigated covering a large range of $(\sin\theta)/\lambda$ values. Nowadays, they are used to test validly the reliability and accuracy obtained by different schemes of calculation. In diamond and germanium, only ten low-order reflections have been investigated leading to a deterioration of the factor of agreement between theory and experiment with respect to that obtained for silicon.

To have access theoretically to charge densities in solid-state physics, *ab initio* calculations have become common only recently. Most use density functional (DF) schemes [1] in conjunction with the plane-wave (PW) basis set technique. One of them is implemented in the program WIEN [2] which is widely distributed and has been used very recently to calculate and compare successfully with experiment the structure factors and charge density of silicon [3]. Other *ab initio* calculations use the Hartree–Fock (HF)–linear combination of atomic orbitals (LCAO) computational scheme whose the most general implementation is given in the program CRYSTAL [4]. The most recent version of this program (CRYSTAL 95) [5] contains a DF option which permits one to take into account to some extent correlation effects through an exchange–correlation potential.

In this work, CRYSTAL 95 has been used to calculate the static and room temperature structure factors and charge densities of diamond, silicon and germanium at the HF and DF

0953-8984/99/305827+17$30.00

levels of theory. They represent an archetype of covalent bonding and it is important to explore the trends of its characteristics when we descend this column of the Periodic Table. Several reasons can be put forward for the choice of diamond, silicon and germanium. As already indicated, the series of the group IV elemental semiconductors can be considered by theorists as one of the best experimental references for electronic structure. This family is very homogeneous, with the same structure (face-centred-cubic lattice with the space group $F_{d\bar{3}m}$). The symmetry is high and the unit cell contains only two atoms. This allows us to impose severe computational conditions ensuring high numerical accuracy in HF calculations. Extended all-electron basis sets can be used and the sophisticated one of silicon shows the quality of the HF structure factors [6] obtained with CRYSTAL. They are accurately optimized to reproduce well experimental ground-state properties such as geometry, bulk modulus, cohesive energy,.

The aim of this study is:

(i) to extend the HF calculations of Pisani *et al* [6] made on silicon to diamond, germanium and to DF schemes not available at that time;
(ii) to compare the results of our calculations to both experimental data and other calculations using non-local basis sets [3, 7] in place of localized functions centred on atoms used in the LCAO method;
(iii) to analyse the differences of the electronic structure deduced from the HF and DF schemes and the effects of the thermal motion on the charge density of each compound.

2. Computational details and theoretical background

2.1. Computational details

2.1.1. The ab initio program. For the present calculations, the CRYSTAL 95 computer program [5] has been used. We refer the reader to a previous paper [8] for a description of the periodic LCAO self-consistent-field computational scheme as implemented in such a code. The CRYSTAL 95 code contains a density functional theory option that permits us to solve self-consistently the Kohn–Sham (KS) equations. The exchange–correlation (XC) potential is expanded in an auxiliary basis set of symmetrized atom-centred Gaussian-type functions (GTFs). In this work, one local and one non-local XC potential have been used. The local potential is indicated by LP: L for LDA (exchange) [9] and P for Perdew–Zunger (correlation) [10] and the non-local or generalized gradient approximation (GGA) potential is indicated by PW for Perdew–Wang (exchange and correlation) [11]. The standard computational conditions for the evaluation of the Coulomb and exchange series, as defined in reference [8], have been used and ensure high numerical accuracy. As regards the reciprocal-space net, a shrinking factor $S = 8$ has been used corresponding to 29 k-points where the Fock matrix is diagonalized.

2.1.2. Basis sets. As regards the basis sets, Bloch functions are constructed from local functions (atomic orbitals) which, in turn, are linear combinations (contractions) of GTFs expressed as the product of a Gaussian and a real solid spherical harmonic.

The carbon basis set [12] can be denoted as a 7-31(1d)G contraction (the first shell is of s type and is a contraction of 7 GTFs, then there are two sp shells and one d shell): it is well adapted to describe the carbon in a tetrahedral structure. The Si and Ge basis sets are 8-841(1d)G and 9-7631(6d,1d)G, respectively. The Si basis set has already been described by Pisani *et al* [6] in the study of the electronic properties of silicon while the Ge basis set has been communicated by Dovesi [12]. The exponents of the most diffuse sp and d shells of each atom have been optimized by searching for the minimum Hartree–Fock crystalline total energy

at the experimental geometry; the following values have been obtained: C: ($\alpha_{sp} = 0.309$, $\alpha_d = 0.808$); Si: ($\alpha_{sp} = 0.129$, $\alpha_d = 0.493$); Ge: ($\alpha_{sp} = 0.155$, $\alpha_d = 0.561$). The same basis sets have been used for the calculations performed with the DF schemes.

2.2. Theoretical background

The static electron density $\rho_0(\vec{r})$ generated by the CRYSTAL code is given by

$$\rho_0(\vec{r}) = \sum_{\vec{g}} \sum_{\mu,\nu} P^{\vec{g}}_{0,\mu\nu} \chi^0_\mu(\mathrm{A}, \vec{r}) \chi^{\vec{g}*}_\nu(\mathrm{B}, \vec{r}) \tag{1}$$

where $\chi^0_\mu(\mathrm{A}, r)$ is the μth AO on atom $\mathrm{A}(r_\mathrm{A})$ in the origin cell, $\chi^g_\nu(\mathrm{B}, r)$ is the νth AO on atom $\mathrm{B}(r_\mathrm{B})$ in the crystal cell associated with the translation g-vector and $P^{\vec{g}}_{0,\mu\nu}$ is the corresponding element of the density matrix.

The method of the calculation of the static $F_0(\vec{s})$ and dynamic $F_T(\vec{s})$ structure factors from $\rho_0(\vec{r})$ has already been reported [13]. The main features of this method can be summarized as follows:

(a) The static structure factor which is the Fourier transform of the unit cell $\rho_0(\vec{r})$ is expressed according to

$$F_0(\vec{s}) = \sum_{\vec{g}} \sum_{\mu\nu} P^{\vec{g}}_{0,\mu\nu} I^{\vec{g}}_{0,\mu\nu}(\vec{s}) \tag{2}$$

where $I^{\vec{g}}_{0,\mu\nu}(\vec{s})$ is the static scattering matrix.

(b) When the atomic vibrations described by the experimental atomic mean square displacement tensors $\langle u^2 \rangle_{ij}$ and treated within the Debye hypothesis are taken into account, the dynamic structure factors are obtained. The expression is formally identical to that for $F_0(\vec{s})$:

$$F_T(\vec{s}) = \sum_{\vec{g}} \sum_{\mu\nu} P^{\vec{g}}_{T,\mu\nu} I^{\vec{g}}_{T,\mu\nu}(\vec{s}) \tag{3}$$

where the element of the dynamic density matrix $P^{\vec{g}}_{T,\mu\nu}$ is expressed as

$$P^{\vec{g}}_{T,\mu\nu} = P^{\vec{g}}_{0,\mu\nu} \frac{I^{\vec{g}}_{0,\mu\nu}(\vec{s}=0)}{I^{\vec{g}}_{T,\mu\nu}(\vec{s}=0)}. \tag{4}$$

The dynamic scattering matrix $I^{\vec{g}}_{T,\mu\nu}(\vec{s})$ includes two types of term. The first ones correspond to couples of orbitals μ, ν centred on the same atom A with $B_{\mathrm{A},xx} = 8\pi^2 \langle u^2_\mathrm{A} \rangle_{xx}$:

$$I^{g_x}_{T,\mu\nu}(s_x) = I^0_{0,\mu\nu}(s_x) \mathrm{e}^{-(1/2)B_{\mathrm{A},xx} s_x^2} \tag{5}$$

where s_x is the x-component of the scattering vector. They are the block-diagonal elements corresponding to the Debye–Waller correction. The second ones constitute the off-block-diagonal elements of the matrix. Their expression is given by

$$I^{g_x}_{T,\alpha^T_x \beta^T_x}(s_x) = \left(\frac{\alpha^T_x}{\alpha}\right)^{n+1/2} \left(\frac{\beta^T_x}{\beta}\right)^{m+1/2} I^{g_x}_{0,\alpha^T_x \beta^T_x}(s_x) \tag{6}$$

with

$$\alpha^T_x = \frac{\alpha}{1 + 2\alpha B_{\mathrm{A},xx}} \qquad \beta^T_x = \frac{\beta}{1 + 2\beta B_{\mathrm{B},xx}}$$

where α and β are exponents of GTFs belonging to orbitals centred on A and B atoms.

3. Results and discussion

3.1. Static structure factors and charge densities

The static structure factors have been calculated from equation (2) at the HF, LP and PW levels for the experimental geometries: $a(\mathrm{C}) = 3.5670$ Å, $a(\mathrm{Si}) = 5.4307$ Å and $a(\mathrm{Ge}) = 5.6579$ Å. The values given in tables 1, 2 and 3 are reported for one atom of the cell:

$$f_0(hkl) = \begin{cases} \dfrac{F_0(hkl)}{8} & \text{for } h+k+l = 4n, 4n+2 \\ \dfrac{F_0(hkl)}{4.2^{1/2}} & \text{for } h+k+l = 4n+1. \end{cases}$$

Table 1. The static atomic scattering factor f_0 of diamond calculated at the HF, LP and PW levels. The lattice parameter is $a = 3.5670$ Å. The experimental values have been listed by Spackman [14] ($B = 0.140$ Å^2). See the text (section 2) for the definition of the HF, LP and PW symbols.

hkl	f_0(HF)	f_0(LP)	f_0(PW)	f_0(exp)
111	3.287	3.294	3.299	3.274
220	1.940	1.967	1.967	1.963
222	0.131	0.100	0.103	0.149
311	1.667	1.700	1.699	1.699
331	1.568	1.558	1.560	1.563
333	1.373	1.376	1.377	1.386
400	1.560	1.569	1.570	1.559
422	1.444	1.441	1.443	1.455
440	1.329	1.324	1.326	1.308
444	1.133	1.127	1.130	—
511	1.396	1.392	1.394	1.411
531	1.283	1.279	1.282	—
533	1.195	1.187	1.191	—
551	1.103	1.097	1.100	—
553	1.020	1.015	1.018	—
555	0.889	0.883	0.887	—
620	1.224	1.218	1.221	—
642	1.051	1.045	1.049	—
660	0.910	0.905	0.909	—
664	0.796	0.791	0.795	—
711	1.100	1.094	1.098	—
731	1.023	1.017	1.021	—
733	0.950	0.945	0.949	—
751	0.887	0.882	0.886	—
753	0.830	0.825	0.829	—
800	0.977	0.971	0.975	—
822	0.910	0.905	0.910	—
840	0.850	0.845	0.849	—
844	0.746	0.742	0.745	—
880	0.587	0.583	0.587	—
911	0.829	0.824	0.827	—

For diamond, the experimental atomic scattering factors are listed by Spackman [14]. They come from the room temperature structure factors of Takama *et al* [15] obtained on synthetic crystals with the Pendellosung technique to which the 222 reflection measured by Weiss and Middleton [16] has been added. The fit of these data with respect to Dawson's model [17] gives

Table 2. The static atomic scattering factor f_0 of silicon calculated at the HF, LP and PW levels. The lattice parameter is $a = 5.4307$ Å. The experimental structure factors are taken from the consolidated set of Cummings and Hart [18] and the Saka and Kato [19] set and corrected for the harmonic thermal factors $B = 0.4668$ Å^2 [3] (a) and $B = 0.4632$ Å^2 [14] (b). See the text (section 2) for the definition of the HP, LP and PW symbols.

				f_0(exp)	
hkl	f_0(HF)	f_0(LP)	f_0(PW)	(a)	(b)
111	10.742	10.720	10.727	10.729	10.728
220	8.651	8.663	8.659	8.657	8.656
222	0.203	0.135	0.151	0.191	0.191
311	8.012	8.036	8.031	8.023	8.020
331	7.268	7.205	7.222	7.251	7.247
333	6.415	6.398	6.406	6.432	6.427
400	7.460	7.440	7.448	7.453	7.449
422	6.725	6.686	6.698	6.721	6.716
440	6.060	6.025	6.036	6.052	6.046
444	4.983	4.959	4.966	4.987	4.979
511	6.459	6.423	6.435	6.443	6.438
531	5.822	5.793	5.803	5.818	5.812
533	5.290	5.261	5.270	5.282	5.275
551	4.818	4.795	4.802	4.815	4.807
553	4.412	4.393	4.399	4.427	4.419
555	3.761	3.749	3.753	3.769	3.760
620	5.477	5.450	5.459	5.472	5.465
642	4.556	4.536	4.543	4.563	4.555
660	3.871	3.856	3.861	3.875	3.866
664	3.356	3.345	3.349	3.354	3.345
711	4.813	4.792	4.799	4.807	4.799
731	4.413	4.395	4.400	4.410	4.402
733	4.064	4.047	4.053	4.076	4.068
751	3.762	3.748	3.752	3.768	3.760
753	3.501	3.490	3.494	3.510	3.501
800	4.188	4.172	4.177	4.185	4.176
822	3.871	3.856	3.861	3.871	3.862
840	3.596	3.583	3.587	3.595	3.586
844	3.147	3.138	3.141	3.144	3.135
880	2.537	2.531	2.533	2.544	2.533
911	3.504	3.492	3.495	3.517	3.508

the harmonic thermal factor $B = 0.140$ Å^2. The dispersion, nuclear scattering and anharmonic (β) corrections are negligible. It can be noted that the Spackman's values (column 5 of table 1) are very similar to those listed by Lu *et al* [7] ($B = 0.1379$ Å^2, $\beta = 0$).

The most complete data set of experimental structure factors of silicon at room temperature has been listed by Zuo *et al* [3]. This list contains 31 reflections taken from the consolidated set of Cummings and Hart [18] and that of Saka and Kato [19]. The observed structure factors were corrected for nuclear scattering ($f_N = 0.0038$ e) and for anomalous dispersion using experimentally derived f'-values [20]. The values given in column 5 of table 2 come from the list of Zuo *et al* [3] after correction for the harmonic thermal factor ($B = 0.4668$ Å^2 [3], values (a) of table 2, and $B = 0.4632$ Å^2 [21], values (b) of table 2). It is noted that the effect of the anharmonic thermal vibration is ignored because the β-value is very uncertain: Deutsch [22] deduces an upper limit of β (0.7 eV Å^{-3}) from an x-ray measurement analysis

Table 3. The static atomic scattering factor f_0 of germanium calculated at the HF, LP and PW levels. The lattice parameter is $a = 5.6579$ Å. The experimental values come from the Matsushita and Kohra [24] and Deutsch, Hart and Cummings [26] data sets after correction for the anomalous dispersion and for the thermal motion $B = 0.5654$ Å^2 [7] (a) and $B = 0.548$ Å^2 [28] (b). See the text (section 2) for the definition of the HF, LP and PW symbols.

				f_0(exp)	
hkl	f_0(HF)	f_0(LP)	f_0(PW)	(a)	(b)
111	27.483	27.493	27.491	27.894	27.883
220	23.680	23.652	23.656	23.766	23.740
222	0.124	0.092	0.095	0.152	0.152
311	22.217	22.167	22.173	22.142	22.109
331	19.524	19.408	19.421	19.482	19.432
333	17.338	17.244	17.255	17.300	17.237
400	20.408	20.312	20.324	20.235	20.191
422	18.096	17.992	18.004	18.040	17.981
440	16.244	16.157	16.168	16.198	16.128
444	13.501	13.447	13.455	13.498	13.410
511	17.348	17.250	17.262	—	
531	15.643	15.564	15.574	—	
533	14.244	14.183	14.191	—	
551	13.092	13.043	13.050	—	
553	12.132	12.092	12.097	—	
555	10.628	10.604	10.608	10.680	10.572
620	14.739	14.671	14.680	—	
642	12.471	12.428	12.434	—	
660	10.874	10.847	10.851	—	
664	9.722	9.705	9.707	—	
711	13.095	13.046	13.052	—	
731	12.128	12.090	12.095	—	
733	11.317	11.287	11.291	—	
751	10.629	10.604	10.608	—	
753	10.045	10.025	10.028	—	
800	11.606	11.573	11.578	—	
822	10.875	10.848	10.852	—	
840	10.253	10.232	10.235	—	
844	9.267	9.253	9.255	—	
880	7.975	7.969	7.970	—	
911	10.045	10.025	10.028	—	

while $\beta = 3.38$ eV Å^{-3} is obtained from the room temperature neutron 222 reflection [23].

For germanium, three accurate data sets are available. They come from experiments of Matsushita and Kohra (MK) [24], Takama and Sato [25] and Deutsch, Hart and Cummings (DHC) [26] made on single crystals. The measured structure factors were corrected theoretically for anomalous dispersion depending on wavelength. The critical analysis of these data made by Lu *et al* [7] shows that the best accuracy corresponds to the MK and DHC measurements. We follow this analysis and give in the column 5 of the table 3 the values of the dynamic structure factors reported by Lu *et al* [7] corrected for the harmonic thermal factor ($B = 0.5654$ eV Å^2 [7], values (a), and $B = 0.548$ eV Å^2 [27], values (b) of table 3). It is noted that these values do not take into account the anharmonic factor β. That is justified since

the corresponding term $\exp(-T_a)$ with

$$T_a = \left(\frac{2\pi}{a}\right)^3 \frac{\langle u^2\rangle^3}{k_B T}\beta_{hkl}$$

(where the symbols have their usual meaning) contributes only 0.2% ($T_a = 2.24 \times 10^{-3}$ K) of the $f_0(h = k = l = 5)$ value with $\beta = 0.9$ eV Å^{-3} [7].

3.1.1. Comparison with experiment. The unweighted factor of agreement

$$R = \sum \left| f_0(\text{exp}) - f_0(\text{theor}) \right| \Big/ \sum f_0(\text{exp})$$

which represents the overall extent of agreement with experiment is given in table 4 for the three models of the calculation. This table shows that the theory–experiment agreement is very satisfactory, especially in the case of silicon when the calculations are made at the HF- and PW-corrected DF levels. For silicon, the quality of the agreement is slightly affected by the B-value which changes only the high-order reflections. The HF structure factors compare very well with experiment especially when the high-order reflections are considered (table 1). When the theoretical f_0-values are obtained from DFT, the agreement deteriorates especially in the case of the LDA-corrected DFT scheme. This is due to a less satisfactory description of the high-order reflections and also to a significant deterioration of the low 222 reflection. This last result looks surprising and will be discussed further. The overall agreement obtained for diamond and germanium is less satisfactory than for silicon. It does not depend on the scheme of calculation. In diamond, the structure factors are rather robust with respect to the B-value [14] and the small values of the structure factors are in part responsible for this result. Low-order reflections (220 and 311 in the HF approach or 111 and 222 in the DFT scheme) also contribute to the deterioration of the R-value. In germanium, the 111 and 222 reflections are not well reproduced with the three methods of calculation. An expansion of the Ge basis set can improve these two structure factors affected by the valence electrons, but before doing this, it would be important to have more experimental reflections.

Table 4. The factor of agreement ($R\% = |f_0(\text{theor}) - f_0(\text{exp})|/\sum f_0(\text{exp})$) between theory and experiment. The values in parentheses are from Zuo *et al* [3] for silicon and from Lu *et al* [7] for diamond and germanium. See the text (section 2) for the definition of the HF, LP and PW symbols.

	HF	LP (LDA)	PW (GGA)
Diamond			
$B = 0.140$ Å^2 [14]	0.96	0.94	0.92
		(0.94)	
Silicon			
$B = 0.4668$ Å^2 [3]	0.15	0.42	0.29
		(0.24)	(0.13)
$B = 0.4632$ Å^2 [22]	0.18	0.31	0.18
		(0.24)	(0.14)
Germanium			
$B = 0.5654$ Å^2 [18]	0.53	0.54	0.52
		(0.43)	
$B = 0.548$ Å^2 [28]	0.73	0.45	0.48
		(0.59)	

3.1.2. Comparison of Hartree–Fock and density functional results. Comparison of the HF f_0-values (column 2) with the DF ones (columns 3, 4) of tables 1, 2, and 3 shows that the behaviour of the low-order reflections differs from that of the high-order ones.

For the *high-order reflections*, the DF formalism calculates f_0-values smaller than the HF ones: the difference is larger with LDA (LP) than with GGA (PW). In the case of diamond, the relative difference

$$\Delta = |f_0(\mathrm{DF}) - f_0(\mathrm{HF})|/f_0(\mathrm{HF})$$

oscillates around a mean value of 0.2% whereas it increases regularly with the decrease of $(\sin\theta)/\lambda$ in silicon and germanium. These factors which are dominated by core electrons are deemed to be better described at the HF level. The loss of accuracy in the calculation of the exchange part of the potential in DF schemes with respect to the HF approach is responsible for this result. The Δ difference is greater in Si and Ge than in diamond and related to the number of core electrons and to their belonging to different shells.

For the *low-order reflections* also influenced by the valence electrons, comparison of HF and DF factors is not so easy. Generally speaking, one expects that DFT which takes into account a part of the electronic correlation is better adapted to describe these reflections than the HF approach in which correlation is fully omitted. If one considers the 222 reflection which is the most important signature of covalent bonding of the group IV solids, that is not verified. No definitive conclusion can be given to account for this surprising result, but a few ideas from other calculations will be examined to clarify this situation for the future. Firstly, in the DFT scheme, the XC potential introduced in the one-electron Kohn–Sham operator is approximated according to a local or gradient correction of the electronic density. From the point of view of the energy, the weight of the correlation part is calculated to be one order of magnitude (or more) smaller than the exchange part. That is also valid for the charge density as shown by Zunger and Freeman [28] for diamond from a self-consistent method used to solve the local density formalism. It is therefore likely, as for the high-order reflections, that the loss of accuracy of the calculation of the exchange part in DFT with respect to the HF approach is not compensated by the introduction of a part of the electronic correlation. To verify this assumption, it is possible now to make with CRYSTAL hybrid calculations by mixing the exact exchange with the correlation taken into account for a LDA or GGA model. Secondly, it is recalled that the basis sets are optimized for the experimental geometry with respect to the HF calculations and kept equal in DF calculations to compare more easily the performances of the two approaches. However, Pisani *et al* [6] have shown that $f_0(222)$ for silicon is rather sensitive to the quality of the basis set. In these conditions, the basis set could be optimized at the DF level and the consequences for the value $f_0(222)$ examined.

HF and DF charge densities have also been calculated to compare the results of the two approaches. The difference (HF–(PW)DF) charge-density (DCHD) map represented on the 110 plane (figure 1) shows similar results for each compound. The symmetry localizes the bond charge at the mid-point of the chemical bond. At this point, HF theory calculates a charge density greater than that of DFT which decreases regularly from 0.10 (diamond) towards 0.02 (germanium) through 0.05 (silicon) e $\mathrm{Å}^{-3}$. There also appears a negative DCHD behind each nucleus along the [111] direction. The positive DCHD around the bond mid-point can be related to the positive difference (HF–DF) of the 222 structure factor. As for structure factors, this positive DCHD is attributable to the fact that, going from the HF to the DF scheme, the charge density is more decreased by the exchange effect than it is increased by the correlation one [28]. The difference map also shows the large anisotropy of the valence charge deformation which has a very diffuse character in the direction perpendicular to the bond. Most of these features also occur in the deformation maps given in figure 3—see later.

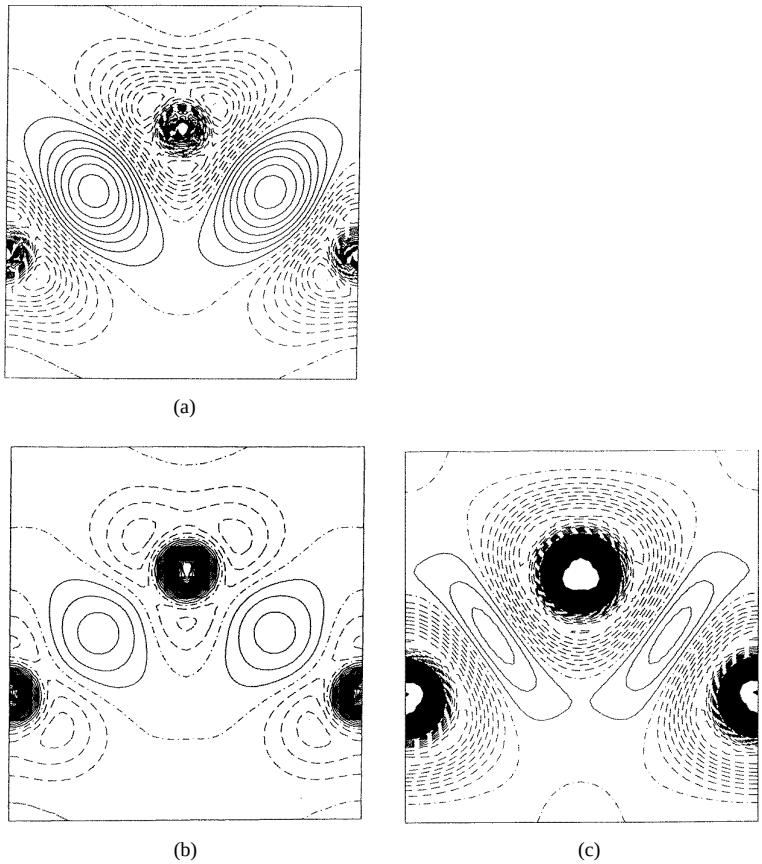

(a)

(b) (c)

Figure 1. The differences between the static HF- and PW-corrected DF charge densities. Full, dashed and dotted–dashed curves indicate positive, negative and zero charge density. The step between two consecutive isodensity curves is 0.002 au for diamond (a) and silicon (b) and 0.001 au for germanium (c).

3.1.3. Comparison with other calculations. Numerous calculations of structure factors and charge densities using different methods and approximations have been reported on the C, Si and Ge series. The results of most of them have already been discussed and compared with the recent ones obtained using the LAPW (LDA or GGA) technique [3, 7]. Here, we limit ourselves to comparing the results from the LAPW [3, 7] and LCAO methods which differ especially in the nature of the basis sets.

The data of table 4 show that both LAPW and LCAO methods lead to an overall agreement with experiment which is very satisfactory and of same quality for diamond and germanium according to the B-value used. The two methods applied to silicon also indicate that the gradient-corrected DF scheme is better than the LDA one. However, for a given XC potential, the experimental structure factors of silicon are better reproduced at the LAPW level even if the difference as regards the LCAO structure factors is very small in the PW–DF scheme.

More precisely, the examination of each reflection (tables 1, 2, 3) shows that the LCAO method calculates structure factors that are systematically smaller than those obtained by the LAPW method at the LDA and GGA levels. This result is valid for each compound. The

five highest-order reflections of diamond provide the only exception to this rule. However, the relative LDA or GGA deviation between LAPW and LCAO structure factors remains very small even for the high-order reflections. For example, one reflection for Ge (555), three reflections for Si (664, 844, 880) and two reflections for C (440, 511) have a deviation higher than 0.5%. Of course, the near-zero value of the 222 structure factor leads to a much larger deviation (10% for C and Si (GGA) and 20% for Ge and Si (LDA)). Given that most of the HF–LCAO structure factors are higher than the LDA or GGA–LAPW ones, the negative differences between the (LDA or GGA) DF–LCAO and corresponding LAPW structure factors are clearly attributable to an approximate evaluation of the exchange potential in DF schemes. The exact calculation of the exchange potential is of primary importance for obtaining the best structure factors in the LCAO method. As already indicated, the use of a hybrid (HF exchange and LDA or GGA correlation) potential in the KS operator will allow one to analyse more appropriately the correlation effects and the comparison between localized (AO) and unlocalized (PW) basis functions to reproduce better the structure factors of the elemental semiconductors. Without these calculations, it can be recalled that in LAPW and LCAO first-principles calculations, similar parameters (number of special k-points in the Brillouin-zone integration, maximum angular momentum for the radial wave functions, plane-wave cut-off (LAPW) or truncation criteria for bielectronic Coulomb and exchange series (LCAO)) determine, after optimization, the accuracy of the results and therefore the convergence of the property. However, the most important parameter used in the two methods is the number of basis functions in which the wave functions are expanded and which limits the size of basis sets. In this work, the numbers of basis functions (atomic orbitals) are 28, 36 and 54 per unit cell for diamond, silicon and germanium, respectively. The reader wishing to appreciate the changes of properties of the ground state of silicon with the number of basis functions is referred to the work of Pisani *et al* [6]. From this study, it appears that the best values of HF structure factors are obtained from the basis set:

(1) where the core electrons are described after reoptimization of core functions carried out for an isolated atom,
(2) where a polarization d function is included (but it is noted that the splitting of the polarization function results in worse agreement with experiment),
(3) where a relatively diffuse sp GTF† is included,
(4) where adding 'ghost' functions at the bond mid-point has no marked effects, contrary to expectation.

These four criteria have been considered for silicon but for diamond and germanium it is necessary to have more numerous experimental reflections before one can validly test any of them.

In summary, the correlation effect is better described in structure factors calculated from the LAPW method than from the LCAO method. Before concluding that the PW basis functions are better adapted than AO basis functions for these calculations, it has to be noted that the XC potential has been fitted in this work according to a predefined 'even-tempered' auxiliary basis set of 8s-type GTFs. Improvement can be obtained with the use of general auxiliary basis sets which are typical for each atom but which are not available at present.

3.1.4. The crystal-field effect. The deviations of the crystal atomic scattering factors and charge densities from those calculated for the free atoms are given in figures 2 and 3, respectively, for the HF approach. To obtain the free-atom wave function, one sp shell has

† It has to be noted that including a diffuse sp GTF, which is not necessarily variationally optimized, limits the computational capabilities of CRYSTAL.

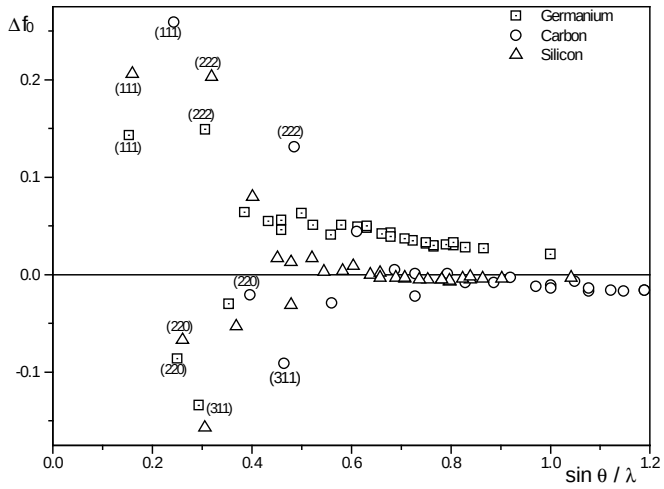

Figure 2. The difference (Δf_0) between the static atomic scattering factor calculated at the HF level for the bulk and the free atom versus $(\sin\theta)/\lambda$.

been added to the crystal basis set and the exponents of the most diffuse sp shells have been reoptimized. In figure 2, only the $f_0 - f_0$(free atom) differences corresponding to the 111, 222, 220 and 311 reflections deviate appreciably from the zero line. The positive difference associated with the 111 reflection expresses the deformation of the electron cloud along the [111] direction while that of the 222 reflection describes the asphericity of the charge density. The largest deformation of the valence electron cloud is observed for diamond while silicon presents the largest asphericity of the charge density. The negative differences corresponding to the 220 and 311 reflections can be explained by the 'pole' deformations of crystalline orbitals in comparison to the free state according to Dawson's model [17] applied to the site symmetry ($\bar{4}3m$: T_d) of the atom. These last features have already been described by Spackman on the basis of the electron distribution in diamond [14] and silicon [21]. Figure 3 reports the map of the deformation of the charge density with respect to the free state on the (110) plane which contains the chemical bond. As expected from the Fourier sum of the experimental $f_0 - f_0$(free atom) differences [14, 21, 27] and from theoretical results [7, 29], these maps give all of the main features of the electronic structure of the crystalline chemical bond and confirm the results deduced from the crystal atomic scattering factors. In the three cases, there is a large build-up of electronic charge along the bonds but the bond charge is much more diffuse in silicon than in diamond or germanium. The deformation of the charge density of diamond is elongated more along the C–C bond, whereas in silicon and germanium, the elongation is perpendicular to the bond. The lack of p core electrons in diamond allows the valence electrons to get nearer the nucleus: this is connected to a monotonic decrease of the total charge density from the atomic position to the mid-point of the bond, whereas in Si and Ge the total charge density is nearly constant (see for example reference [7]). The observed peaks at the bond mid-points and the deficits behind the nuclei along the [111] direction are 0.42 and -0.22 e Å^{-3} for C, 0.21 and -0.11 e Å^{-3} for Si and 0.11 and -0.07 e Å^{-3} for Ge. These results compare very well with the experimental data: 0.41 and -0.19 e Å^{-3} for C [14], 0.21 and -0.09 e Å^{-3} [21] or 0.22 and -0.07 e Å^{-3} [22] for Si and 0.17 and -0.05 e Å^{-3} for Ge [27]. They also confirm and improve very slightly on the accurate results of recent calculations obtained from the all-electron LAPW implementation of the local density formalism (0.45, -0.13 e Å^{-3}) for

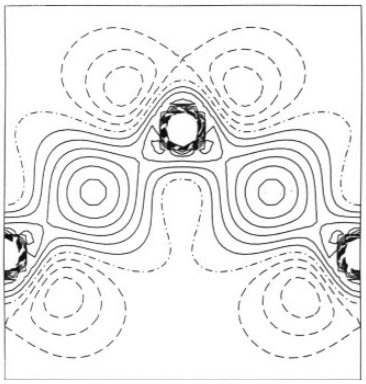

(a)

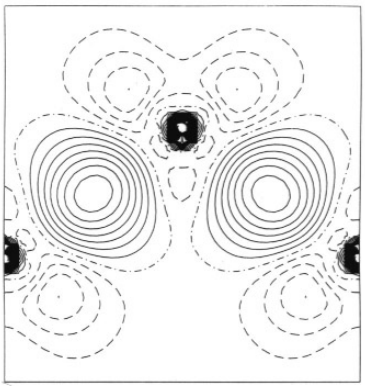

(b)

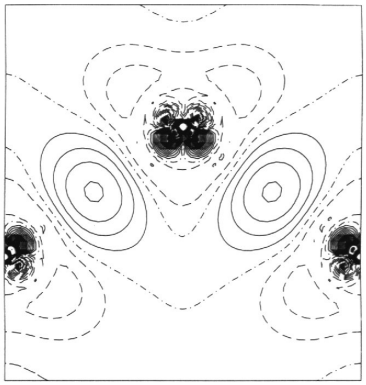

(c)

Figure 3. Deformation maps of the static electron charge density on the 110 plane calculated at the HF level. Full, dashed and dotted–dashed curves indicate positive, negative and zero charge density, respectively. The step between two consecutive isodensity curves is 0.01 au for diamond (a) and 0.004 au for silicon (b) and germanium (c).

C [7], (0.18, -0.10 e Å^{-3}) [7] or (0.189 e Å^{-3}) [3] for Si and (0.13, -0.05 e Å^{-3}) for Ge [7] or the Perdew–Wang 91 generalized gradient approximation (PW91 GGA) (0.194 e Å^{-3}) for Si [3].

3.2. Thermal motion effects

The room temperature scattering factors f_T have been calculated using the equations (3) to (6) with the harmonic factors given in section 3.1. The values are given in tables 5, 6 and 7 for diamond, silicon and germanium, respectively. They are not very different from those deduced from the Debye–Waller expression. This indicates that the off-block-diagonal elements of the dynamic scattering matrix (equation (6)) are very small with respect to the block-diagonal ones and that the orbital overlapping coming from different atoms is negligible at this temperature.

In order to show accurately the effects of the thermal motion, the dynamic HF charge densities have been calculated for each compound. The difference between room temperature

Table 5. The room temperature atomic scattering factor f_T of diamond calculated at the HF, LP and PW levels according to equation (3) with $B = 0.140$ Å^2 [14]. See the text (section 2) for the definition of the HF, LP and PW symbols.

hkl	f_T(HF)	f_T(LP)	f_T(PW)
111	3.259	3.267	3.271
220	1.896	1.922	1.922
222	0.129	0.099	0.101
311	1.615	1.647	1.645
331	1.489	1.479	1.481
333	1.273	1.276	1.278
400	1.491	1.500	1.500
422	1.351	1.348	1.350
440	1.217	1.212	1.214
444	0.993	0.987	0.990
511	1.296	1.291	1.294
531	1.165	1.161	1.164
533	1.062	1.055	1.058
551	0.958	0.953	0.956
553	0.867	0.862	0.865
555	0.723	0.718	0.722
620	1.096	1.091	1.094
642	0.901	0.896	0.899
660	0.747	0.742	0.746
664	0.624	0.621	0.624
711	0.956	0.951	0.954
731	0.869	0.864	0.868
733	0.790	0.786	0.789
751	0.721	0.717	0.720
753	0.660	0.656	0.659
800	0.819	0.814	0.817
822	0.747	0.742	0.745
840	0.682	0.678	0.681
844	0.573	0.569	0.572
880	0.413	0.410	0.413
911	0.660	0.656	0.659

and $T = 0$ charge densities is deduced and given in figure 4. As expected, the deformation of the charge density is very small and affects especially the electron distribution along the [111] direction. The thermal motion of the atoms decreases the charge density around the nucleus but also in the bond area for silicon and germanium, making the valence charge more diffuse. However, in silicon, a very slight increase in charge density can be observed along the Si–Si bond showing 'bond' peaks of only 1.10^{-3} e Å^{-3} slightly shifted from the bond mid-point towards the nuclei. The thermal motions of silicon and germanium are therefore very similar as also indicated by their close values of the harmonic B-factor. In the case of diamond, the difference between room temperature and $T = 0$ charge densities remains positive throughout the valence area. This result is different from that obtained for silicon and germanium but, as in silicon, it shows 'bond' peaks of 610^{-3} e Å^{-3} slightly shifted towards the nuclei. The thermal motion in diamond seems to include at room temperature several atoms closely linked. This allows us to understand better the small value of the B-factor with respect to those of Si and Ge which would be attributable to a large bond charge density and to its delocalization along both the short C–C bond and around the nucleus.

Table 6. The room temperature atomic scattering factor f_T of silicon calculated at the HF, LP and PW levels according to equation (3) with $B = 0.4668$ Å^2 [3]. See the text (section 2) for the definition of the HF, LP and PW symbols.

hkl	f_T(HF)	f_T(LP)	f_T(PW)
111	10.615	10.593	10.600
220	8.381	8.393	8.389
222	0.195	0.131	0.145
311	7.672	7.696	7.691
331	6.744	6.685	6.702
333	5.767	5.752	5.760
400	7.004	6.986	6.993
422	6.118	6.082	6.094
440	5.343	5.310	5.321
444	4.124	4.104	4.110
511	5.808	5.774	5.786
531	5.070	5.045	5.054
533	4.464	4.440	4.448
551	3.940	3.921	3.926
553	3.496	3.480	3.486
555	2.796	2.787	2.790
620	4.676	4.654	4.661
642	3.651	3.635	3.641
660	2.912	2.901	2.906
664	2.370	2.362	2.366
711	3.935	3.917	3.924
731	3.496	3.480	3.486
733	3.121	3.106	3.106
751	2.800	2.786	2.785
753	2.523	2.513	2.511
800	3.254	3.240	3.239
822	2.914	2.901	2.900
840	2.622	2.611	2.610
844	2.154	2.146	2.144
880	1.530	1.525	1.521
911	2.525	2.515	2.513

4. Conclusions

New LCAO–SCF calculations using both HF and LDA- or GGA-corrected DF schemes have been reported for diamond, silicon and germanium; these were carried out to obtain $T = 0$ and room temperature structure factors and charge densities. The agreement with experiment is very satisfactory and of similar quality to that obtained recently with the LAPW method. The best agreement is obtained with the Hartree–Fock approach. This is particularly attributable to the contribution of high-order reflections. In density functional theory where the gradient (PW) correction of the electronic density reproduces the experimental structure factors better than the local correction, the improvement of HF low-order structure factors is not as expected. On the contrary, the low 222 reflection which is the most important signature of covalent bonding in these semiconductors has been deteriorated. The DF–LCAO structure factors are smaller than those calculated within the HF approach. They are also systematically smaller than the corresponding LAPW ones. The exact calculation of the exchange potential, as done in the HF approach, is therefore of primary importance even for low-order reflections more sensitive to

Table 7. The room temperature atomic scattering factor f_T of germanium calculated at the HF, LP and PW levels according to equation (3) with $B = 0.5654$ Å^2 [7]. See the text (section 2) for the definition of the HF, LP and PW symbols.

hkl	f_T(HF)	f_T(LP)	f_T(PW)
111	27.126	27.134	27.132
220	22.856	22.830	22.833
222	0.123	0.091	0.094
311	21.159	21.112	21.118
331	17.955	17.848	17.860
333	15.391	15.307	15.317
400	19.014	18.925	18.936
422	16.278	16.184	16.195
440	14.105	14.030	14.039
444	10.923	10.880	10.886
511	15.399	15.312	15.323
531	13.405	13.337	13.345
533	11.781	11.731	11.737
551	10.452	10.414	10.419
553	9.351	9.320	9.324
555	7.632	7.615	7.617
620	12.359	12.297	12.304
642	9.739	9.706	9.711
660	7.913	7.894	7.896
664	6.592	6.581	6.582
711	10.456	10.417	10.422
731	9.347	9.318	9.322
733	8.421	8.397	8.400
751	7.633	7.616	7.618
753	6.963	6.950	6.951
800	8.750	8.725	8.729
822	7.914	7.895	7.897
840	7.202	7.188	7.189
844	6.066	6.057	6.058
880	4.532	4.529	4.529
911	6.964	6.950	6.952

the correlation effects. Next, hybrid calculations taking into account both exact HF exchange and correlation parts of the potential will have to be carried out to confirm this conclusion.

Both DF–LAPW and LCAO methods calculate with an excellent accuracy the experimental structure factors of elemental semiconductors. However, the use of the plane-wave basis functions is very slightly better adapted than the localized atomic orbitals basis set in the density functional approach to describe this property. In spite of this, all of the main features are well reproduced, such as the confirmation of the low 222 DFT value which looks basis set independent. At this stage, it is noted how a similar study extended to other (insulator, molecular, ...) compounds would be useful to generalize these results and to confirm the trend of the HF approach giving better structure factors than the DF schemes.

In charge-density maps, the HF approach enhances the calculated bond charge around the bond mid-point with respect to the DF scheme. It reports more accurately the valence charge deformation in the form of the values of the build-up of charge at the bond mid-point and of the deficit of charge occurring behind each nucleus along the [111] direction. The room temperature structure factors calculated within our orbital model are very close to

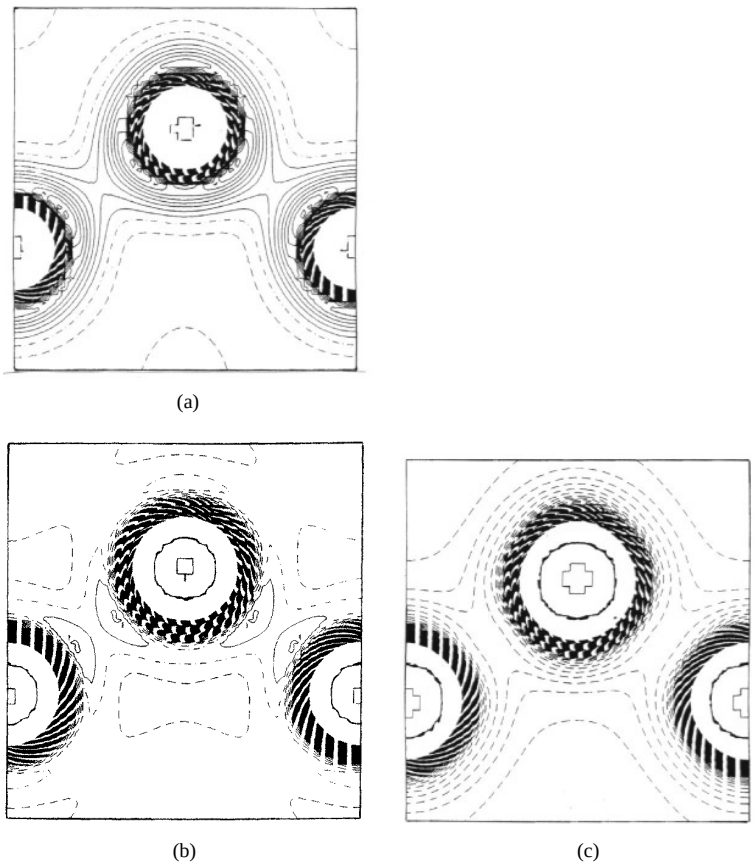

(a)

(b) (c)

Figure 4. The thermal motion effect. The differences between the room temperature and static bulk HF charge densities. Full, dashed and dotted–dashed curves indicate positive, negative and zero charge density, respectively. The step between two consecutive isodensity curves is 0.0001 au for diamond (a), silicon (b) and germanium (c).

those obtained with the Debye–Waller formula. The overlapping between orbitals centred on different atoms is therefore negligible. The charge density of diamond, both around the atom and along the chemical bond, is larger at room temperature than at $T = 0$. With respect to those in silicon and germanium, the thermal motion in diamond is different. It seems to involve more than a single atom, as both the large charge density along the C–C bond and the small value of the B-factor also indicate.

References

[1] Hohenberg P and Kohn W 1964 *Phys. Rev.* B **136** 864
Kohn W and Sham L J 1965 *Phys. Rev.* A **140** 1133
[2] Blaha P, Schwarz K, Soratin P and Trickey S B 1990 *Comput. Phys. Commun.* **59** 399
Blaha P, Schwarz K, Dufek P and Augustyn R 1995 *WIEN95* Technical University of Vienna
[3] Zuo J M, Blaha P and Schwarz K 1997 *J. Phys.: Condens. Matter* **9** 7541
[4] Dovesi R, Pisani C, Roetti C, Causà M and Saunders V R 1989 *CRYSTAL 88 Program No 577* Quantum Chemistry Program Exchange, Indiana University, Bloomington, IN

[5] Dovesi R, Saunders V R, Roetti C, Causà M, Harrison N M, Orlando R and Aprà E 1996 *CRYSTAL 95 User's Manual* University of Torino
[6] Pisani C, Dovesi R and Orlando R 1992 *Int. J. Quantum Chem.* **42** 5
[7] Lu Z W, Zunger A and Deutsch M 1993 *Phys. Rev.* B **47** 9385
[8] Pisani C, Dovesi R and Roetti C 1988 *Hartree–Fock ab initio Treatment of Crystalline Systems (Springer Lecture Notes in Chemistry vol 48)* (Heidelberg: Springer)
[9] Dirac P A M 1930 *Proc. Camb. Phil. Soc.* **26** 376
[10] Perdew J P and Zunger A 1981 *Phys. Rev.* B **23** 5048
[11] Perdew J P 1991 *Electronic Structure of Solids* ed P Ziesche and H Esching (Berlin: Akademie)
Perdew J P, Chevary J A, Vosko S H, Jackson K A, Pederson M R, Singh D J and Fiolhais C 1992 *Phys. Rev.* B **46** 6671
Perdew J P, Burke K and Wang Y 1996 *Phys. Rev.* B **54** 16 533
[12] Dovesi R 1997 Private communication
[13] Azavant P, Lichanot A, Rerat M and Chaillet M 1994 *Theor. Chim. Acta* **89** 213
Azavant P, Lichanot A, Rerat M and Pisani C 1996 *Int. J. Quantum Chem.* **58** 419
[14] Spackman M A 1991 *Acta Crystallogr.* A **47** 420
[15] Takama T, Tsuchiya K, Kobayashi K and Sato S 1990 *Acta Crystallogr.* A **46** 514
[16] Weiss R J and Middleton R 1965 Private communication to B Dawson
[17] Dawson B 1967 *Proc. R. Soc.* A **298** 264
Dawson B 1967 *Proc. R. Soc.* A **298** 379
[18] Cummings S and Hart M 1988 *Aust. J. Phys.* **41** 423
[19] Saka T and Kato N 1986 *Acta Crystallogr.* A **42** 469
[20] Deutsch M and Hart M 1984 *Phys. Rev.* B **30** 640
Deutsch M and Hart M 1988 *Phys. Rev.* B **37** 2701
[21] Spackman M A 1986 *Acta Crystallogr.* A **42** 271
[22] Deutsch M 1992 *Phys. Rev.* B **45** 646
[23] Roberto J, Batterman B and Keating D 1974 *Phys. Rev.* B **9** 2590
Keating D, Nunes A, Batterman B and Hastings J 1971 *Phys. Rev.* B **4** 2472
[24] Matsushita T and Kohra K 1974 *Phys. Status Solidi* **24** 531
[25] Takama T and Sato S 1981 *Japan. J. Appl. Phys.* **20** 1183
[26] Deutsch M, Hart M and Cummings S 1990 *Phys. Rev.* B **42** 1248
[27] Brown A S and Spackman M A 1990 *Acta Crystallogr.* A **46** 381
[28] Zunger A and Freeman J 1977 *Phys. Rev.* B **15** 5049
[29] Orlando R, Dovesi R, Roetti C and Saunders V R 1990 *J. Phys.: Condens. Matter* **2** 7769